Journal of Industrial Microbiology & Biotechnology (2002) 29, 361 – 367

www.nature.com/jim

Biofilm material properties as related to shear-induced deformation and detachment phenomena

P Stoodley[1,2,3], R Cargo[1,4], CJ Rupp[1,4], S Wilson[1] and I Klapper[5]

[1]*Center for Biofilm Engineering, Montana State University, Bozeman, MT 59717, USA;* [2]*Department of Civil Engineering, Montana State University, Bozeman, MT 59717, USA;* [3]*Department of Microbiology, Montana State University, Bozeman, MT 59717, USA;* [4]*Department of Industrial and Mechanical Engineering, Montana State University, Bozeman, MT 59717, USA;* [5]*Department of Mathematical Sciences, Montana State University, Bozeman, MT 59717, USA*

Biofilms of various *Pseudomonas aeruginosa* strains were grown in glass flow cells under laminar and turbulent flows. By relating the physical deformation of biofilms to variations in fluid shear, we found that the biofilms were viscoelastic fluids which behaved like elastic solids over periods of a few seconds but like linear viscous fluids over longer times. These data can be explained using concepts of associated polymeric systems, suggesting that the extracellular polymeric slime matrix determines the cohesive strength. Biofilms grown under high shear tended to form filamentous streamers while those grown under low shear formed an isotropic pattern of mound-shaped microcolonies. In some cases, sustained creep and necking in response to elevated shear resulted in a time-dependent fracture failure of the ''tail'' of the streamer from the attached upstream ''head.'' In addition to structural differences, our data suggest that biofilms grown under higher shear were more strongly attached and were cohesively stronger than those grown under lower shears.
Journal of Industrial Microbiology & Biotechnology (2002) **29,** 361–367 doi:10.1038/sj.jim.7000282

Keywords: biofilm; detachment; hydrodynamics; shear stress; strength; viscoelastic fluid

Introduction

Microbial biofilms accumulate on virtually all submerged surfaces in industrial and natural environments. The bacterial cells in the biofilm are typically surrounded by a protective extracellular polymeric slime (EPS) matrix that also provides the biofilm with mechanical stability [6]. In industrial pipelines, biofilms can cause accelerated corrosion of steel surfaces, increased pressure drops, and product contamination and spoilage. Detachment of cells from biofilms in food production facilities and drinking water systems may result in the potential transmission of pathogens *via* contaminated food [32], drinking water [21], or aerosols [30]. In medical devices, such as dental unit water lines [22] or ventilators [8], the growth and subsequent detachment of bacteria from biofilms have the potential to increase the risk of pathogen exposure to patients. Further, the mode of biofilm detachment will determine how an infection or contamination is disseminated and the success to which it is controlled. In flowing systems, interactions between the water (the bulk fluid) and attached biofilms will depend on the hydrodynamics and the mechanical properties of the biofilm. Although a moving fluid will create a drag force on biofilm structures, which protrude into the bulk fluid, the usual assumption is that the shear force created as the fluid flows over a surface is the principle physical force acting on the biofilm. To understand, predict, and manipulate how a biofilm will behave in response to fluid shear, it is necessary to know something about the mechanical properties of biofilms. This is particularly important in optimizing mechanical techniques for removing biofilms from surfaces, a desirable goal for many industries.

Correspondence: Dr Paul Stoodley, 366 EPS Building, Montana State University, Bozeman, MT 59717, USA
Received 6 February 2002; accepted 13 June 2002

Very little is known about the material properties of biofilms or how they are influenced by the growth environment. This is due to two main reasons. First, only a few groups have recognized the importance and implications of viewing biofilms as materials; second, biofilms are very difficult to test mechanically. Unlike conventional materials like solids, which can be molded into uniform test pieces, or fluids, for which defined volumes can be poured between rheometer plates, biofilms are nonuniform, microscopically small, and attached to surfaces. Testing of scraped biofilm will inevitably disrupt the sample. When testing any material, it is important to use procedures that are relevant to the physical environment in which the material is to be exposed. While rheometer testing of scraped biofilm suspensions has provided useful fundamental data [18], for biofilms growing in flowing systems, it is appropriate to test under fluid shear.

We have designed an *in vitro* flow cell model for growing biofilms under a wide range of controlled hydrodynamic conditions and have used digital time lapse microscopic (DTLM) imaging to observe and quantify biofilm deformation in response to fluid shear [24,26]. Using these techniques, we were able to conduct tests analogous to stress–strain and creep tests on attached biofilms. These studies demonstrated that various mixed and pure culture aerobic and anaerobic biofilms had a complex rheology, which was dependent on the fluid shear at which the biofilm was grown and changes in the ionic environment. Koerstgens *et al* [14] found similar results for biofilms tested under normal compressive stresses [5,6]. These experimental data have been modeled using the principle of associated polymeric systems [15,23] in which biofilms were described as viscoelastic Jeffreys fluids, interpreted in terms of the various chemical and physical interactions between the matrix polymers [12]. The viscous component to this model allows us to interrogate time-dependent deformation in response to shear over different scales.

In this paper, we discuss some of the methods that we have used to investigate the influence of shear on biofilm detachment and deformation and relate the mechanical properties of biofilms to mechanisms of adhesive and cohesive failure. Although the data presented are drawn from experiments conducted on various strains of *Pseudomonas aeruginosa*, the purpose of the present study is to demonstrate various biofilm responses to shear rather than directly compare differences or similarities between strains.

Materials and methods

Biofilm reactor system

Biofilms were grown in square glass flow cells (3 mm wide, 3 mm deep, and 200 mm long; BST-3-50; Friedrich and Dimmock, Millville, NJ), which were incorporated into a recirculating loop fed from a mixing vessel (Figure 1). The various components were connected by silicone rubber tubing. Nutrients were delivered by peristaltic pump (Masterflex; Cole Parmer, Niles, IL) and the recycle flow rate was controlled with a vane head pump (Masterflex; Cole Parmer). The nutrient influent flow rate was set at 4.3 ml/min to give a resulting dilution rate (D=1.5 h^{-1}) above washout to minimize the planktonically growing population and favor biofilm growth. The highest maximum specific growth rate for all of the strains used in this study was 0.70 h^{-1} (doubling time of 1 h) from 24 separate shake flask growth curves with a minimum of at least three runs for each strain. A septum-sealed sampling port was positioned between two flow breaks in the effluent line. The flow cells were positioned on the stage of either an upright Olympus BH2 microscope or an inverted Zeiss Axiovert 100 microscope without interrupting flow.

Flow cell hydrodynamics

The average flow velocity (u) through each flow cell was measured using in-line flow meters (McMillan Flo-Sensor model 101T # 3724; Cole Parmer). The Reynolds number (Re) in the flow cells and the fluid shear stress at the wall (τ_w) for laminar and turbulent flows were calculated using the flow velocity and flow cell geometry and described in detail elsewhere [27]. The transition between laminar and turbulent flow occurred at a Reynolds number (Re) of 1200 (u=0.33 m/s). Biofilms were grown at a range of flow rates from Re of 8 (u_g=0.002 m/s, τ_{wg}=0.03 N/m^2) up to 3600 (u_g=1 m/s, τ_{wg}=5.09 N/m^2). The hydrodynamic conditions during biofilm growth are denoted by subscript g, i.e., Re_g and τ_{wg}. Under operating conditions, the water temperature in the reactor system was maintained at either 28 or 37°C. Appropriate temperature corrections were made for calculation of hydrodynamic parameters.

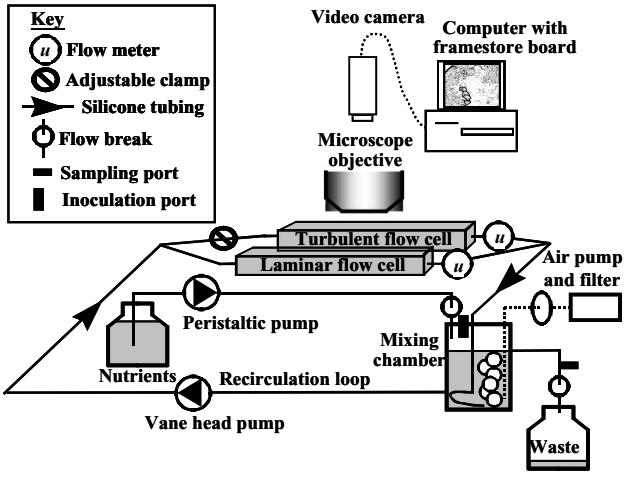

Figure 1 Experimental system used for growing biofilms. Biofilms were observed in square glass flow cells.

Reactor sterilization

Most of the reactor system and nutrients were autoclave-sterilized. Heat-sensitive components were sterilized using a method adapted from Fisher and Petrini [5] by exposing to 70% ethanol for 15 min, 40% NaOCl solution (approximately 12% available chlorine when undiluted) for 15 min, and again to 70% ethanol for 15 min. To verify sterility, three 0.1-ml aliquot effluent samples were plated onto King's B agar after the flow system had been run with sterile media for 3 days prior to inoculation.

Inocula and nutrients

Biofilms were grown from various *P. aeruginosa* strains. Strains and growth media are given in Table 1. After inoculation into the mixing chamber, the system was run as a batch culture with recirculating flow for 24 h before switching to continuous culture mode with nutrient feed and overflow. Biofilms were grown for up to 14 days.

Image analysis

A COHU 4612-5000 CCD camera (COHU, San Diego, CA) and a Scion VG-5 PCI framestore board (Scion, Frederick, MD) were used to capture time lapse and "snapshot" images. Image processing and analysis was done using Scion Image (free download available from www.scioncorp.com/index.htm). A 1-mm graticule with 10-μm divisions (Ref. no. CS990; Graticules, Tonbridge, Kent, UK) was used for calibration. In addition to direct observation, biofilms were also stained with the activity stain 5-cyano-2,3-ditolyl tetrazolium chloride (CTC) (0.02% wt/vol final concentration) for 30 min at 30°C [31]. Biofilms were observed using epifluorescence with an excitation wavelength of 400–500 nm and a 590-nm barrier filter.

Scanning electron microscopy (SEM)

SEM was performed on *P. aeruginosa* PAN067 biofilms grown under laminar and turbulent flow to investigate the influence of flow on biofilm structure. One-centimeter sections of the laminar and turbulent flow cells were fixed in a 5% glutaraldehyde cacodylate buffer (0.1 M) solution for 10 min at room temperature. The samples were then dehydrated in a 30%, 50%, 70%, and 100% ethanol series for 3 min each. The sample was then air-dried for 1 day in a dessicator. Wall sections of the square glass tubing were cut out with a diamond knife and mounted on a conducting coupon for sputter coating with gold palladium. The samples were viewed on a Leica Stereoscan 100 SEM at 10, 15, or 25 kV acceleration voltage.

Shear-induced deformation and detachment

Creep curves: After the growth period of constant fluid shear, the biofilms were subjected to variations in shear by adjusting the

Table 1 *P. aeruginosa* strains and growth media

Strain	Reference	Relevant genotype or phenotype	Growth medium
PAO1	[7]	Prototrophic, nonmucoid opportunistic pathogen	Minimal salts medium (MSM) with 400 ppm glucose [24]
PAO-JP1	[19]	Δ*las*Itet, *Las*I null mutant derived from PAO1; does not produce the cell signaling molecule *N*-3-oxo-dodecanoyl homoserine lactone (OdDHL)	1/50 Luria broth
PAN067	[10]	Elastase-negative mutant deficient in the production of the cell signalling molecule *N*-butanoyl-L-homoserine lactone (BHL)	MSM with 400 ppm glucose [24]
FRD1	[17]	Mucoid cystic fibrosis isolate	MSM with sodium glutamate (13 mg/l)

flow rate in the flow cells. For creep tests, the τ_w was elevated and then held for periods of up to 1 h before reducing back to τ_{wg} or 0. The resulting deformation on biofilm microcolonies was quantified by measuring the strain (ε) in the longitudinal direction. In the present study, ε is defined as the ratio of the change in length of a microcolony (or the change in length between two fiducial points within a microcolony) to the original length (before changing τ_{wg}).

Stress–strain curves: These tests were similar to the creep tests, but instead of holding the elevated τ_w for an extended period of time, τ_w was increased (loading) then decreased (unloading) in a stepwise manner with step intervals of approximately 5 s. The corresponding ε was measured from the microscopic images. An apparent shear modulus, E_{app} (a measure of biofilm rigidity), was calculated from the linear region of the resulting stress–strain curves. We refer to an "apparent" elastic modulus to distinguish our parameter from the conventional elastic or Young's modulus, which is calculated from the relationship between ε and a normal compressive or tensile stress in the linear or Hookean region of the stress–strain response. Additionally, in our system, although we relate the deformation of biofilm to the theoretical fluid shear stress, the actual forces acting on the biofilm are a combination of both normal and shear forces caused by complex local flow patterns associated with the irregular biofilm structures. Calculated parameter values from these tests are, therefore, approximate.

Shear-induced detachment: For the biofilm detachment, assay flow was first turned off so that τ_w was 0. The τ_w was then incrementally stepped up in 1-min intervals until either all of the cells had been washed away or the maximum flow rate was achieved (prior to the onset of leaks). Time lapse images taken at 10-s intervals were used to count the concentration of single cells

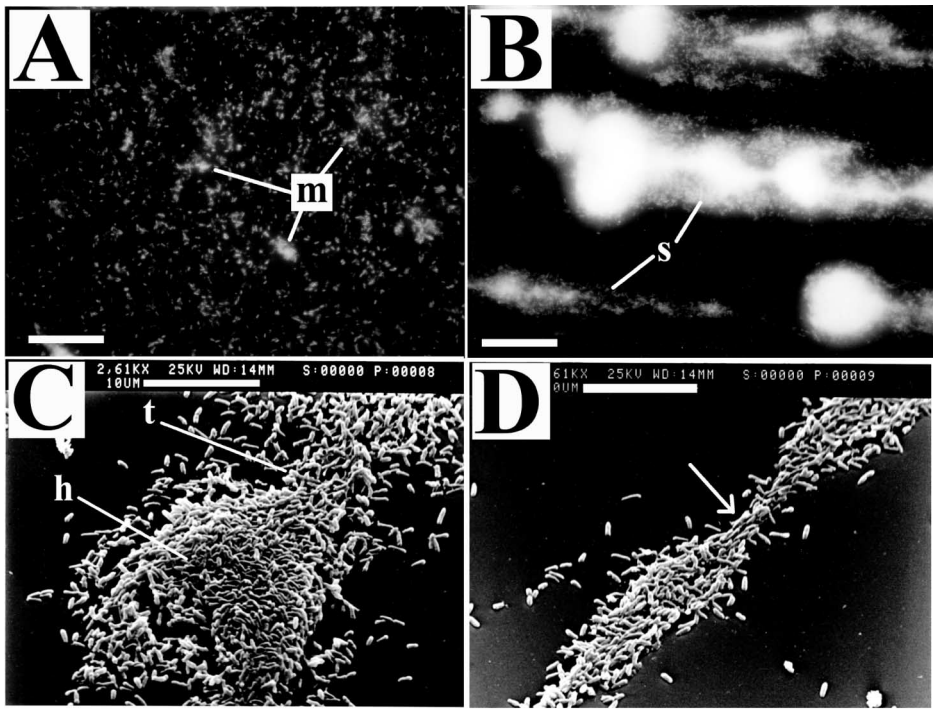

Figure 2 *P. aeruginosa* PANO67 biofilm grown under laminar or turbulent flow (u=0.033 and 1 m/s, respectively). (A) Biofilm grown under laminar flow stained with CTC consisting of small mound-shaped microcolonies (m) and single cells. (B) Biofilm grown in turbulent flow stained with CTC. The biofilm developed filamentous streamers (s), which were elongated in the downstream direction. The microcolonies were much larger than those grown in laminar flow but there were fewer single cells attached to the exposed substratum between the microcolonies. In both cases, flow was from left to right. (C) SEM showing the attached "head" (h) of the streamer and the start of the downstream tail (t). (D) The filamentous streamer "tail." Individual cells in the tail appeared to be aligned in the downstream direction (arrow). Under flowing conditions, the tails were free to oscillate in the flow. Flow was from bottom left to upper right. Scale bars=40 μm for (A) and (B) and 10 μm for (C) and (D).

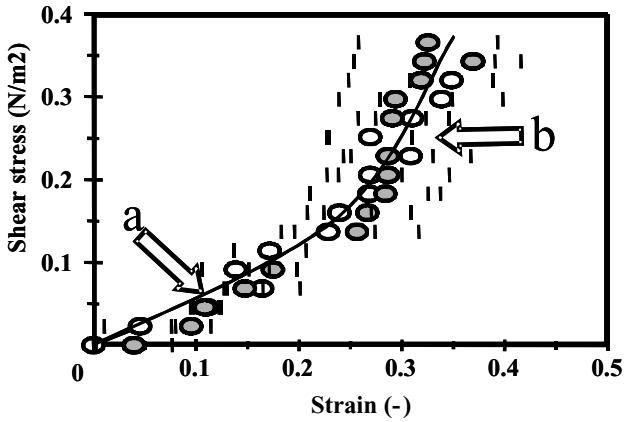

Figure 3 Stress–strain curve from a JP1 cell cluster grown under laminar flow with a τ_{wg} of 0.005 N/m^2. The open circles are the loading part of the curve and the closed circles and the unloading portion. The curve shows that the biofilm gave a nonlinear elastic response when subjected to elevated fluid shear over a short time period. An apparent elastic modulus (E_{app}) of approximately 1 N/m^2 was found from the low shear stress region "a." The higher modulus region "b" had a shear modulus of approximately 2 N/m^2.

(or microcolonies) on the surface while τ_w was increased. A detachment rate coefficient (k_{det}) was calculated by dividing the number of cells that had detached during each 1-min increment by the number of cells on the surface immediately prior to increasing the τ_w.

Results

Biofilm structure

The *Pseudomonas* biofilms grown under laminar flow generally consisted of hemispherical mound-shaped microcolonies, which formed an isotropic pattern on the surface. In the channels between the microcolonies, individual cells could be seen attached to the glass surface (Figure 2A). The biofilm microcolonies grown in turbulent flow, however, were elongated in the downstream direction to form filamentous streamers (Figure 2B). The streamers were attached to the glass substratum by an upstream "head" while the downstream "tails" were free to oscillate in the flow.

Stress–strain curves

The stress–strain curves for all the *Pseudomonas* strains showed an elastic response when subjected to elevated fluid shear over short time scales (in seconds). The curves generally had an initially low shear modulus at low strains, which increased with increasing shear stress (Figure 3). Some curves were sigmoidal, suggesting that in these cases, a yield point had been reached (data not shown). The shear modulus for the various biofilms varied from 1 to 280 N/m^2. Linear regression of the grouped data from all of the *Pseudomonas* strains showed that E_{app} increased with τ_{wg}. The empirical formulas were $E_{app}=10.8\tau_{wg}+7.8$, $r^2=0.75$, $n=17$ for regression of the linear data and $E_{app}=30.3\tau_{wg}^{0.58}$, $r^2=0.87$ for regression of the log–log data [12]. A video sequence "*Pseudomonas aeruginosa* FRD1 biofilm elasticity" showing the elastic response to increasing and decreasing fluid shear is available at http://www.erc.montana.edu/Res-Lib99-SW/movies/.

Creep curves

The creep curves showed that after the initial elastic strain in response to the elevation in fluid shear, there was a linear viscous response as the biofilm flowed over time (Figure 4A). For biofilms grown under turbulent flow ($\tau_{wg}=5.3$ N/m^2), when the τ_w was reduced to 0 N/m^2 after the load period of 30 min, there was an instant elastic recoil. A resulting negative strain indicated that at the τ_{wg}, an inherent tension had developed in the biofilm streamer during growth. When the shear was returned to the τ_{wg}, there was a residual strain. The experimental creep curves presented the classic creep response of a viscoelastic fluid. The viscosity was found from

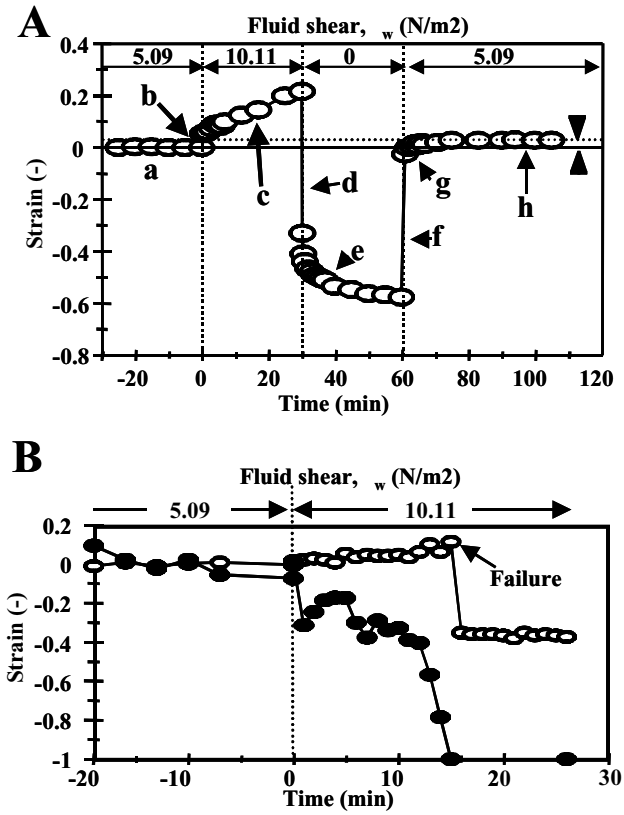

Figure 4 Creep curves from PAO1 biofilms grown under turbulent flow ($\tau_{wg}=5.3$ N/m^2) showing different responses. (A) The curve can be broken down into distinct portions for interpretation. (a) The streamer length was steady for at least 30 min prior to applying an elevated load, giving us confidence that any elongation would be due to elastic stretching and not merely from growth. When the τ_w was raised to 10.11 N/m^2, there was immediate elastic stretching (b). The associated E_{app} was 66.7 N/m^2. The length of the streamer then increased linearly with time, demonstrating viscous flow (c). When the τ_w was reduced to 0 N/m^2, there was an instant elastic recoil (d) followed by a time-dependent creep recovery (e). The negative strain (i.e., the streamer had contracted to less than its original length) demonstrates that during growth, the biofilm streamer had developed an inherent tension in the matrix. (f) When the τ_w was returned to the τ_{wg}, again there was an immediate elastic response ($E_{app}=85$ N/m^2) followed by time-dependent creep extension (g). After approximately 10 min, the streamer length had stabilized with a residual strain of 0.04 h, indicating that the deformation was permanent and that the biofilm had flowed like a viscous fluid. (B) In this case, the biofilm streamer broke after 14 min of the loading period at τ_w 10.11 N/m^2. The open circles represent the strain associated with the elongation of the streamer during creep and the closed circles are the negative strain associated with the width of the streamer at the break point.

the induced residual strain caused by the increased shear over the load period. Data from four separate experiments gave a biofilm viscosity of $3.6\times10^5\pm2.6\times10^5$ (mean±1 SD) N s/m^2. However, in some cases, the biofilm cell cluster failed before the load period was finished. The failure was either from detachment of the whole cell cluster (adhesive failure) or from the breaking off of a streamer tail (cohesive failure). By monitoring the length of the streamer and the width of the streamer at the break point, it was clear that the biofilms underwent "necking," a phenomenon seen in the failure of many ductile materials (Figure 4B). A video sequence "Shear-induced creep and detachment of *Pseudomonas aeruginosa* PAO1 biofilm streamer" is available for viewing at http://www.erc.montana.edu/Res-Lib99-SW/movies/.

Shear-induced detachment

Detachment of single bacterial cells from the surface of 6-day-old *P. aeruginosa* PAO1 biofilms grown in laminar (u_g=0.03 m/s) or turbulent flow (u_g=1.0 m/s) was monitored as u was incrementally increased from 0 m/s (Figure 5). Monitoring was conducted in spaces between cell clusters in which single cells could be clearly distinguished to facilitate tracking the detachment process. In the biofilm grown at u=0.03 m/s, there was no detachment until u was increased to 1 m/s. As u was elevated, cells rapidly detached in a fashion similar to that of a classic washout curve (Figure 5A). For the biofilm grown at 1 m/s, there was no significant detachment until u was increased to 2.5 m/s (Figure 5B). However, in this case, the rate of detachment was less than for the biofilms grown at low shear. This is illustrated in Figure 5C, which shows the detachment rate coefficient (k_{det}) as a function of increasing u for both biofilms. As expected, the k_{det} increased with flow velocity for both biofilms. For u above 2 m/s, k_{det} for the biofilm grown in turbulent flow was approximately 10 times that for the biofilm grown in laminar flow. However, it should be cautioned that as fewer cells remain on the surface, k_{det} will become increasingly influenced by the detachment of only a few cells over the time increment. The detachment of whole biofilm cell clusters showed a similar shaped detachment curve as that for single cells (data not shown). Data grouped from previous experiments using both pure and defined mixed and undefined mixed culture biofilms suggest that the onset of detachment of cell clusters occurs when the shear is increased to approximately twice that at which the biofilm was formed. Regression analysis yielded the empirical formula: $\tau_{det}=2.3\tau_{wg}$, $r^2=0.81$, $n=8$. A video sequence "Shear-induced detachment of *Pseudomonas aeruginosa* PAO1 biofilm cells from a glass surface" is available at http://www.erc.montana.edu/Res-Lib99-SW/movies/.

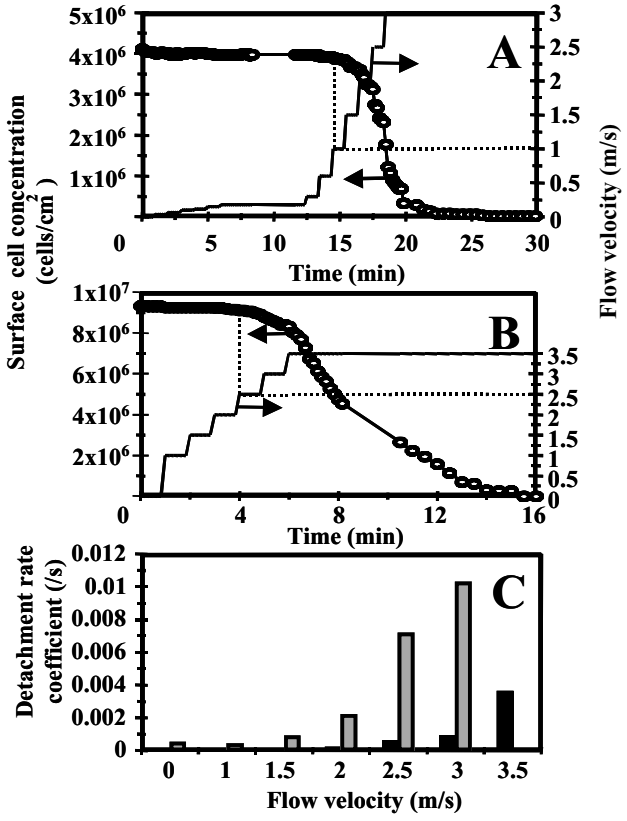

Figure 5 Shear-induced detachment of cells from *P. aeruginosa* biofilms grown at laminar (A) or turbulent flow (B). The onset of detachment for the biofilm grown under laminar flow (u_g=0.33 m/s) occurred at u=1 m/s but at 2.5 m/s for the biofilm grown under turbulent flow (u_g=1.0 m/s). (C) Kinetic parameters such as detachment rate coefficients can be calculated from these curves showing that biofilm cells that had attached under higher shear (filled bars) were more firmly attached than those which attached under low shear (hatched bars). This type of shear-induced detachment assay may be a useful tool for determining the relative adhesion strength of biofilms formed on different surfaces or environmental conditions.

Discussion

By investigating deformation and detachment of biofilm structures caused by fluctuations in fluid shear, we have been able to demonstrate on the microscopic scale that the attached *Pseudomonas* biofilms behaved like viscoelastic fluids. Over short time periods (seconds) of exposure to elevated shear, the biofilms demonstrated a nonlinear elastic response. But over longer time scales, they demonstrated viscous flow. In terms of response and rigidity, the biofilms were similar to the pedal mucus of slugs [3] or sputum from cystic fibrosis patients [11]. The viscoelastic nature of biofilms may explain the formation of ripple structures that developed in mixed species biofilms grown under turbulent flow. Time lapse sequences demonstrated that the ripples flowed downstream, along the channel walls of the flow cell [25]. The flow of biofilms across surfaces may represent a largely unrecognized dissemination mechanism in industrial pipelines and medical devices. For example, Inglis [8] noted the formation of "wave-like patterns" in biofilms formed in tracheal tubes and hypothesized that the possible flow of biofilms was related to biofilm detachment and dissemination into the lungs. Koerner [13] also noted the "infective, highly viscous and adhesive layers" that formed inside endotracheal tubes and hypothesised that shear-induced detachment from this layer caused by respiratory gasflow may cause infective particles to travel into the lower airway, increasing pathogenicity.

The present study also suggests that biofilms grown under higher shear are more strongly adhered and have a stronger EPS matrix than those grown under lower shear. Busscher *et al* [2] reported that the conditions under which initial attachment occurred determined the attachment strength of oral *Streptococcus* spp. Similarly, it has been reported that biofilm density was directly related to the fluid shear during growth [28], although work by Peyton [20] suggests that increased density may be more related to the increased transport of nutrients rather than shear stress.

However, it is clear that hydrodynamics conditions not only influence the structure of biofilms but also the material properties. This may be explained in terms of polymer chemistry and the physical arrangement of individual polymer strands in the biofilm EPS matrix [6]. It is possible that at higher shear, as the biofilm is stretched out, the polymer strands become physically aligned and pulled closer, allowing more chance for electrostatic interactions and hydrogen bonding, much like the strength imparted to a rope by the spinning together of weak individual fibers. This would explain the "J"-shaped curves we observed in the stress–strain tests Figure 3 a common phenomenon of biological materials [29]. The formation of filamentous streamers, which form at high shear both in the laboratory and in the natural environment such as the filamentous prokaryotic mats found in hot springs [9] and acid mine drainage runoff [4], certainly imply some type of structural alignment. Although the physical arrangement of polymers in the biofilm may explain differences in biofilm strength, it is also possible that biofilms regulate their strength in response to their physical environment. This could be through increased EPS production as suggested by Applegate and Bryers [1] or by regulating metabolic pathways in response to shear [16]. The strength of the biofilm could also be regulated by varying the chain length of EPS polymers or by polymer modification such as the *O*-acetylation of alginate, which influences structure in *P. aeruginosa* biofilms [17]. Another possibility is that high shear environments select for subpopulations that have higher substratum-binding affinities and produce stronger biofilms. In this case, it is interesting to speculate on the use of differential shear environments to select for populations with mechanical properties that may be of industrial relevance.

In this paper, we have discussed biofilm material properties and how they can be related to biofilm behavior and shear-induced detachment mechanisms through both adhesive and cohesive failure. The development of the new field of biofilm mechanics will not only further our understanding of the fundamental behaviors of biofilms, particularly in flowing systems, but will also be an important factor in linking structure to function. It will ultimately help answer the question of whether or not biofilms are coordinated entities that actively regulate their structure in response to variations in their physical environment.

Nomenclature

ε	mechanical strain (–)
E_{app}	apparent elastic modulus (N/m^2)
k_{det}	detachment rate coefficient (s^{-1})
Re	Reynolds number (–)
τ_w	fluid shear stress at the wall (N/m^2)
τ_{det}	fluid shear at the onset of detachment of biofilm cell clusters (N/m^2)
τ_{wg}	fluid shear stress at which the biofilm was grown (N/m^2)
u	average flow velocity (m/s)
u_g	flow velocity at which the biofilm was grown (m/s)

Acknowledgements

This work was funded by the National Institutes of Health RO1 grant GM60052-02 and the WM Keck foundation. From MSU, we thank Dr. Michael Franklin for experimental discussion and for providing FRD1.

References

1 Applegate DH and JD Bryers. 1991. Effects of carbon and oxygen limitations and calcium concentrations on biofilm removal processes. *Biotechnol Bioeng* 37: 17–25.
2 Busscher HJ, R Bos and HC Vandermei. 1995. Initial microbial adhesion is a determinant for the strength of biofilm adhesion. *FEMS Microbiol Lett* 128: 229–234.
3 Denny MW. 1984. Mechanical properties of pedal mucus and their consequences for gastropod structure and performance. *Am Zool* 24: 23–36.
4 Edwards KJ, PL Bond, TM Gihring and JF Banfield. 2000. An archaeal iron-oxidizing extreme acidophile important in acid mine drainage. *Science* 287: 1796–1799.
5 Fisher PJ and O Petrini. 1992. Fungal saprobes and pathogens as endophytes of rice (*Oryza sativa* L.). *New Phytol* 120: 137–143.
6 Flemming H-C, J Wingender, C Mayer, V Koerstgens and W Borchard. 2000. Cohesiveness in biofilm matrix polymers. In: Allison D, P Gilbert, HM Lappin-Scott and M Wilson (Eds), Community Structure and Cooperation in Biofilms. SGM Symposium Series 59. Cambridge Univ. Press, Cambridge, pp. 87–105.
7 Holloway BW, V Krishnapillai and AF Morgan. 1979. Chromosomal genetics of *Pseudomonas*. *Microbiol Rev* 43: 73–102.
8 Inglis TJJ. 1993. Evidence for dynamic phenomena in residual tracheal tube biofilm. *Br J Anaesth* 70: 22–24.
9 Jahnke LL, W Eder, R Huber, JM Hope, KU Hinrichs, JM Hayes, VJ Des Marais da, SL Cady and RE Summons. 2001. Signature lipids and stable carbon isotope analyses of octopus spring hyperthermophilic communities compared with those of aquificales representatives. *Appl Environ Microbiol* 67: 5179–5189.
10 Jones S, B Yu, NJ Bainton, M Birdsall, BW Bycroft, SR Chhabra, AJR Cox, P Golby, PJ Reeves, S Stephens, MK Winson, GPC Salmond, GSAB Stewart and P Williams. 1993. The lux autoinducer regulates the production of exoenzyme virulence determinants in *Erwinia carotovora* and *Pseudomonas aeruginosa*. *EMBO J* 12: 2477–2482.
11 King M, B Dasgupta, RP Tomkiewicz and NE Brown. 1997. Rheology of cystic fibrosis sputum after *in vitro* treatment with hypertonic saline alone and in combination with recombinant human deoxyribonuclease I. *Am J Respir Crit Care Med* 156: 173–177.
12 Klapper I, CJ Rupp, R Cargo, B Purvedorj and P Stoodley. 2002. A viscoelastic fluid description of bacterial biofilm material properties. *Biotechnol Bioeng* 80(3): 289–296.
13 Koerner RJ. 1997. Contribution of endotracheal tubes to the pathogenesis of ventilator-associated pneumonia. *J Hosp Infect* 35: 83–89.
14 Koerstgens V, HC Flemming, J Wingender and W Borchard. 2001. Influence of calcium ions on the mechanical properties of a model biofilm of mucoid *Pseudomonas aeruginosa*. *Water Sci Technol* 43: 49–57.
15 Leiber L, M Rubinstein and RH Colby. 1991. Dynamics of reversible networks. *Macromolecules* 24: 4701–4707.
16 Liu Y and JH Tay. 2000. Metabolic response of biofilm to shear stress in fixed-film culture. *J Appl Microbiol* 89: 564–572.
17 Nivens DE, DE Ohman, J Williams and MJ Franklin. 2001. Role of alginate and alginate o-acetylation in the formation of *Pseudomonas aeruginosa* microcolonies and biofilms. *J Bacteriol* 183: 1047–1057.
18 Ohashi A and H Harada. 1994. Adhesion strength of biofilm developed in an attached-growth reactor. *Water Sci Technol* 29: 281–288.
19 Pearson JP, EC Pesci and BH Iglewski. 1997. Roles of *Pseudomonas aeruginosa* las and rhl quorum-sensing systems in control of elastase and rhamnolipid biosynthesis genes. *J Bacteriol* 179: 5756–5767.
20 Peyton BM. 1996. Effects of shear-stress and substrate loading rate on *Pseudomonas aeruginosa* biofilm thickness and density. *Water Res* 30: 29–36.
21 Piriou P, S Dukan, Y Levi and PA Jarrige. 1997. Prevention of bacterial growth in drinking water distribution systems. *Water Sci Technol* 35: 283–287.
22 Putnins EE, D Di Giovanni and AS Bhullar. 2001. Dental unit waterline contamination and its possible implications during periodontal surgery. *J Periodontol* 72: 393–400.
23 Rubinstein M and AV Dobrynin. 1997. Solutions of associative polymers. *Trends Polym Sci* 5: 181–186.
24 Stoodley P, Z Lewandowski, JD Boyle and HM Lappin-Scott. 1999.

Structural deformation of bacterial biofilms caused by short term fluctuations in flow velocity: an *in situ* demonstration of biofilm viscoelasticity. *Biotechnol Bioeng* 65: 83–92.
25 Stoodley P, Z Lewandowski, JD Boyle and HM Lappin-Scott. 1999. The formation of migratory ripples in a mixed species bacterial biofilm growing in turbulent flow. *Environ Microbiol* 1: 447–457.
26 Stoodley P, A Jacobsen, BC Dunsmore, B Purevdorj, S Wilson, HM Lappin-Scott and JW Costerton. 2001. The influence of fluid shear and $AlCl_3$ on the material properties of *Pseudomonas aeruginosa* PAO1 and *Desulfovibrio* sp. EX265 biofilms. *Water Sci Technol* 43: 113–120.
27 Stoodley P, L Hall-Stoodley and HM Lappin-Scott. 2001. Detachment, surface migration, and other dynamic behavior in bacterial biofilms revealed by digital time-lapse imaging. *Methods Enzymol* 337: 306–319.
28 Vieira MJ, LF Melo and MM Pinheiro. 1993. Biofilm formation: hydrodynamic effects on internal diffusion and structure. *Biofouling* 7: 67–80.
29 Vincent J. 1990. Structural Biomaterials, revised edition. Princeton Univ. Press, Princeton, NJ.
30 Walker JT, CW Mackerness, D Mallon, T Makin, T Williets and CW Keevil. 1995. Control of *Legionella pneumophila* in a hospital water-system by chlorine dioxide. *J Ind Microbiol* 15: 384–390.
31 Walsh S, HM Lappin-Scott, H Stockdale and BN Herbert. 1995. An assessment of the metabolic activity of starved and vegetative bacteria using two redox dyes. *J Microbiol Methods* 24: 1–9.
32 Zottola EA and KC Sasahara. 1994. Microbial biofilms in the food industry — should they be a concern? *Int J Food Microbiol* 23: 125–148.